

## Research Note

# The nature of the unusual source IRAS 18530+0817\*

H.J. Walker<sup>1</sup>, V. Tsikoudi<sup>2</sup>, C.A. Clayton<sup>1</sup>, T. Geballe<sup>3</sup>, D.H. Wooden<sup>4</sup>, and H.M. Butner<sup>5</sup>

<sup>1</sup> CLRC, Rutherford Appleton Laboratory, Chilton, Didcot, Oxon, OX11 0QX, UK

<sup>2</sup> University of Ioannina, Dept. of Physics, 45 110 Ioannina, Greece

<sup>3</sup> Joint Astronomy Centre, 660 N A'ohoku Place, Hilo, Hawaii 96720, USA

<sup>4</sup> NASA Ames Research Center, Moffett Field, CA 94035, USA

<sup>5</sup> Dept. of Terrestrial Magnetism, Carnegie Institution of Washington, 5241 Broad Branch Road, Washington, DC 20015, USA

Received 15 March 1996 / Accepted 15 January 1997

**Abstract.** Infrared photometry and spectroscopy of the unassociated (infrared-only) IRAS source, IRAS 18530+0817, indicate that it is a highly unusual evolved star surrounded by a dense envelope of cool gas and dust. The IRAS data reveal a large infrared excess and significant flux variability in the 12 – 25  $\mu\text{m}$  region, as well as a prominent, silicate emission feature at 8.5 – 11.5  $\mu\text{m}$ . The shape of the feature also appears to vary; in 1993 it was apparently attenuated by an absorption with a sharp edge at 9.5  $\mu\text{m}$ , which may be circumstellar or photospheric in origin. At other times the silicate feature appears to be self-absorbed by varying amounts. Near-infrared spectra of IRAS 18530+0817 are dominated by steam absorptions, with the K-band spectrum showing only a narrow band of relatively unabsorbed continuum at 2.15 – 2.29  $\mu\text{m}$ . The object appears to possess the strongest stellar photospheric H<sub>2</sub>O absorptions yet observed. We tentatively conclude that the central star of IRAS 18530+0817 is a late-type, O-rich, AGB star (a Mira variable) surrounded by an envelope of O-rich dust.

**Key words:** circumstellar matter – stars: IRAS 18530+0817 – stars: evolution – stars: mass-loss – stars: AGB and post-AGB – infrared: stars

## 1. Introduction

During the course of a study of flare stars (Tsikoudi, 1988) at the IRAS wavebands, we came across the bright source IRAS 18530+0817, which had not been optically identified. The IRAS Low Resolution Spectrum (IRAS LRS) of this source has strong silicate emission peaking near 9  $\mu\text{m}$ , which is either

self-absorbed near 10  $\mu\text{m}$  or whose profile is affected by another spectral feature. Figure 1 shows the LRS spectra of IRAS 18530+0817 and three other sources with different types of silicate feature. Z Pup (IRAS 07304–2032), Fig. 1b, and IRAS 17050–4123, Fig. 1d, have strong silicate emission features with blue continua (LRS class 29). These spectra show the normal location of the silicate emission feature, peaking around 9.6  $\mu\text{m}$  to 10  $\mu\text{m}$ . RAFGL 5146S (IRAS 17482–2824), Fig. 1c, has a self-absorbed silicate emission feature (LRS class 42) with peaks around 8.5 and 11.5  $\mu\text{m}$ . The possibly unusual silicate feature in IRAS 18530+0817 prompted us to investigate this source further. The source is so faint in the blue and red wavebands that it is not seen on the Palomar B and R plates. Using a finding chart of the area around the IRAS position we made follow-up observations of this object at red and infrared wavelengths, at the South African Astronomical Observatory (SAAO) and the Mauna Kea Observatories (Hawaii) respectively. In this paper we discuss our observations as well as those in the literature and we attempt to understand and determine the nature of this source and its dust shell.

The IRAS LRS Atlas (1986) did not place the spectrum in the normal O-rich classes, but labelled it 04, “strange band shape”. There are only 12 sources classed as 04; two of these look similar to IRAS 18530+0817. Cheeseman et al. (1989) classified the LRS spectra using Artificial Intelligence techniques, where spectra which were judged “similar” to each other, using Bayesian statistics, were put into the same class. They placed the spectrum of IRAS 18530+0817 in one of the less common silicate emission feature classes, namely epsilon 1 ( $\epsilon 1$ ), with the spectra of 137 other objects. These stars have weak emission features in addition to silicate emission, high variability, and some members are thought to be supergiants with thick dust shells. Of these 137 objects, about 80 show a feature around 8.5 – 11.5  $\mu\text{m}$  which is very similar to IRAS 18530+0817. There are also some objects in the IRAS LRS Atlas with a similar spectral

---

Send offprint requests to: H. J. Walker

\* Based on observations from IRAS, UKIRT, IRTF and SAAO.

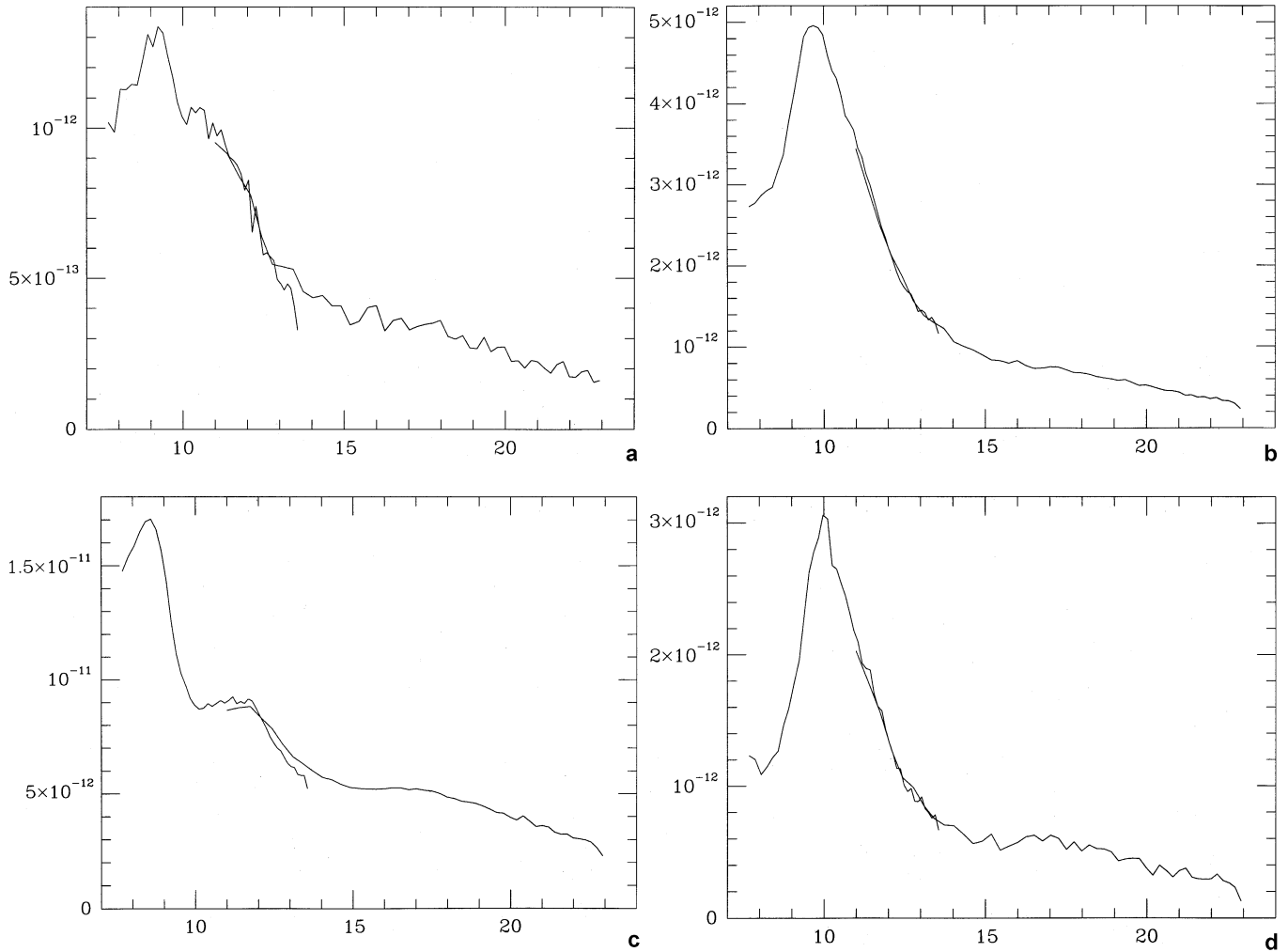


**Fig. 1a–d.** IRAS LRS Spectra of: **a** IRAS 18530+0817, class 04 (AI class  $\epsilon$ 1), **b** Z Pup, class 29 (AI class  $\beta$ 1), **c** RAFGL 5146S, class 42 (AI class  $\zeta$ 4), **d** IRAS 17050-4123, class 29 (AI class  $\beta$ 11). The unit of flux is  $\text{W m}^{-2} \mu\text{m}^{-1}$ .

**Table 1.** Observing Log for IRAS 18530+0817

UT date	Telescope	Instrument	Wavelength $\mu\text{m}$	Resolving power	Standard
19930525	UKIRT	CGS3	7.5 – 13.4	60	HR 7001
19941002	UKIRT	CGS4	2.15 – 2.36	650	HR 7061
19950517	UKIRT	CGS4	1.85 – 2.52	850	HR 7354
19950519	UKIRT	CGS4	1.01 – 1.35	920	HR 7167
19950618	IRTF	HIFOGS	7.7 – 13.5	200	HR 5340
19950618	UKIRT	CGS3	8.7 – 10.3	200	HR 7001
19950619	IRTF	HIFOGS	7.9 – 13.7	200	HR 5340
19950619	UKIRT	CGS3	7.5 – 13.3	60	HR 7001
19950820	UKIRT	CGS3	7.4 – 13.2	60	HR 7001

shape not placed in the  $\epsilon$  class. Z Pup and IRAS 17050–4123, in Fig. 1, belong to the pure silicate emission feature classes, the beta classes ( $\beta$ 1 and  $\beta$ 11 respectively).

More than 40 catalogues which contain celestial objects were searched when compiling the IRAS PSC in order to iden-

tify the IRAS detections with known sources. The identification given for IRAS 18530+0817 was EIC 719. The Equatorial Infrared Catalog (EIC) contains sources which were observed at  $2.7\mu\text{m}$  during an infrared survey in 1977 (Sweeney et al., 1978). EIC 719 was observed for the first time during this survey. There was a  $2.7\mu\text{m}$  flux measurement for EIC 719 but no further information nor an identification given. Kastner et al. (1993) gave H, K, L photometry for IRAS 18530+0817.

IRAS 18530+0817 was included in the radio-survey of IRAS sources which searched for OH molecules at 1612 MHz with Arecibo radio telescope (Lewis et al., 1990). There was no positive detection for this object. Another survey of IRAS sources, searching for CO at mm wavelengths (Kastner et al., 1993) found a marginal detection for IRAS 18530+0817, in the (2-1) transition but not in the (1-0) transition. They also detected SiO from the source. The ROSAT database was examined, but only an upper limit could be determined for the source. Kastner et al. (1993) reported that they could not estimate a distance based on their models of kinematic distances and measured velocities because the  $V_{l,SR}$  was not consistent with its position in

**Table 2.** Photometric variability of IRAS 18530+0817

Time UTCS sec	IRAS PASS2 CRDD fluxes				IRAS LRS
	12 $\mu$ m Jy	25 $\mu$ m Jy	60 $\mu$ m Jy	100 $\mu$ m Jy	$\log_{10}(F_{12})$ $W m^{-2} \mu m^{-1}$
71613594.9	49.4 $\pm$ 0.1	46.7 $\pm$ 0.1	6.7 $\pm$ 0.5	10.4 $\pm$ 9.0	-11.97
72295587.1	49.0 $\pm$ 0.1	43.4 $\pm$ 0.1	5.6 $\pm$ 0.6	–	-11.88
88074085.2	31.3 $\pm$ 0.1	34.1 $\pm$ 0.1	4.6 $\pm$ 0.3	–	–
88166820.4	22.0 $\pm$ 0.1	33.1 $\pm$ 0.1	4.6 $\pm$ 0.3	9.5 $\pm$ 7.5	-12.18

The IRAS fluxes in columns 2 – 5 are measured very accurately, using PASS2 CRDD. The errors in the measurement are given, overall the uncertainty in calibration dominates (see IRAS Explanatory Supplement). IRAS PSC fluxes: 43.75Jy, 34.24Jy, 5.77Jy, < 85Jy.

the sky. Loup et al. (1993) estimated the distance to be 1.9kpc, using a standard luminosity for their sample of objects. They reported a mass loss rate for IRAS 18530+0817 of  $1 \times 10^{-6} M_{\odot} yr^{-1}$  and an expansion velocity of 12 km s $^{-1}$ .

## 2. Observations

The observations presented here were undertaken to complement and extend existing data, to assist in understanding the nature of the source. In particular, these new observations consist of 0.7 and 1.03  $\mu$ m photometry and spectroscopy at 1.01 – 1.35, 1.84 – 2.51, and 7 – 13  $\mu$ m.

CCD photometry was undertaken with the 1.0m telescope of the South African Astronomical Observatory at Sutherland on 18th July 1991. A region centered on the IRAS position was observed in the U, V, R and I bands. Only one object was visible within (or indeed even close to) the IRAS 95% confidence error ellipse (15''  $\times$  4'' towards P.A. 80°). This object is at 18h 53m 0.9s, +08° 17' 21'' (1950.0), some 5.5'' from the IRAS position, and was only detectable in the I band. Hence, this is an infrared only object.

A log containing details of all the spectral observations made is shown in Table 1. Several observations were made using the United Kingdom Infrared Telescope (UKIRT) on Mauna Kea, some as part of the UKIRT Service programme. Two instruments were used; the 1 – 5  $\mu$ m spectrometer (CGS4) and the 10 – 20  $\mu$ m spectrometer (CGS3). All spectra were sampled every 1/3 resolution element. Reduction of the CGS4 data, which were obtained in a stare/nod mode, involved ratioing by spectra of standard stars of spectral types A and F (after removal of the atomic hydrogen absorption lines in the J and K bands), flux calibration, and wavelength calibration using an Argon arc. The J band spectrum is shown in Fig. 2a and the more extensive of the two K band spectra is shown in Fig. 2c. All CGS3 spectra were obtained in a chop/nod mode, with a chopper throw of 20'' EW and a chop frequency of 5Hz. Data reduction was similar to that for CGS4. Wavelength calibration was achieved with a Krypton lamp. The resultant spectrum, obtained on 25 May 1993, is shown in Fig. 2b. This spectrum has been slightly smoothed by convolving the data with a Gaussian of FWHM 1.5 data points.

Two spectra in the 7 – 13  $\mu$ m region were taken on 18 and 19 June 1995 with HIFOGS (Witteborn et al., 1991) on the NASA Infrared Telescope Facility (IRTF). Both spectra were done in

**Table 3.** Photometry and line observations of IRAS 18530+0817

PHOTOMETRY		Wavelength	Flux	Data	
Filter band	$\mu$ m	$W m^{-2} \mu m^{-1}$	Source		
R	0.70	< 4.0 $\times 10^{-16}$	1		
I	0.90	3.0 $\times 10^{-15}$	1		
H	1.65	5.2 $\times 10^{-12}$	2		
K	2.20	8.8 $\times 10^{-12}$	2		
CGS4	2.25	6.6 $\times 10^{-12}$	1		
2.7	2.70	9.0 $\times 10^{-12}$	3		
L	3.60	8.8 $\times 10^{-12}$	2		
CGS3	10	1.9 $\times 10^{-12}$	1		
IRAS PSC	12	4.6 $\times 10^{-13}$	4		
IRAS PSC	25	6.8 $\times 10^{-14}$	4		
IRAS PSC	60	2.3 $\times 10^{-15}$	4		
IRAS PSC	100	< 8.5 $\times 10^{-15}$	4		
LINES		Frequency	Temperature	Velocity	Data
Molecule	GHz	$T_B$ (K)	km.s $^{-1}$	Source	
OH	1.612	–	–	5	
SiO	43	0.29	-3.2	2	
CO (1-0)	115	< 0.06	–	2	
CO (2-1)	230	0.0625	-5	2	

Data sources: 1 – Present work; 2 – Kastner et al, 1993; 3 – Sweeney et al, 1978; 4 – IRAS PSC (1987); 5 – Lewis et al, 1990.

a chop and nod mode, with a chopper throw of 20'' EW and a chop frequency of 10Hz. The channel resolution was 0.05 microns/pixel. The two spectra are shifted by 3.5 channels to provide Nyquist sampling and to fill any missing channels. The flux calibration was done relative to  $\alpha$  Boo, and an atmospheric correction was applied to remove the telluric and ozone features. This was done to each spectrum separately, and the quality of the fit can be seen in the small ozone residual at 9.4 $\mu$ m. The data from 19 June were scaled by 0.8 to match those from 18 June, and the combined spectrum is shown in Fig. 2d.

## 3. Results

All the information which is currently available for IRAS 18530+0817 is shown in Tables 2 and 3, and in Figs. 1, 2 and 3. There is no detection of OH at 1612 MHz, but the SiO maser line is detected at 43GHz, and the CO line is just detected at 230GHz, but not at 115GHz.

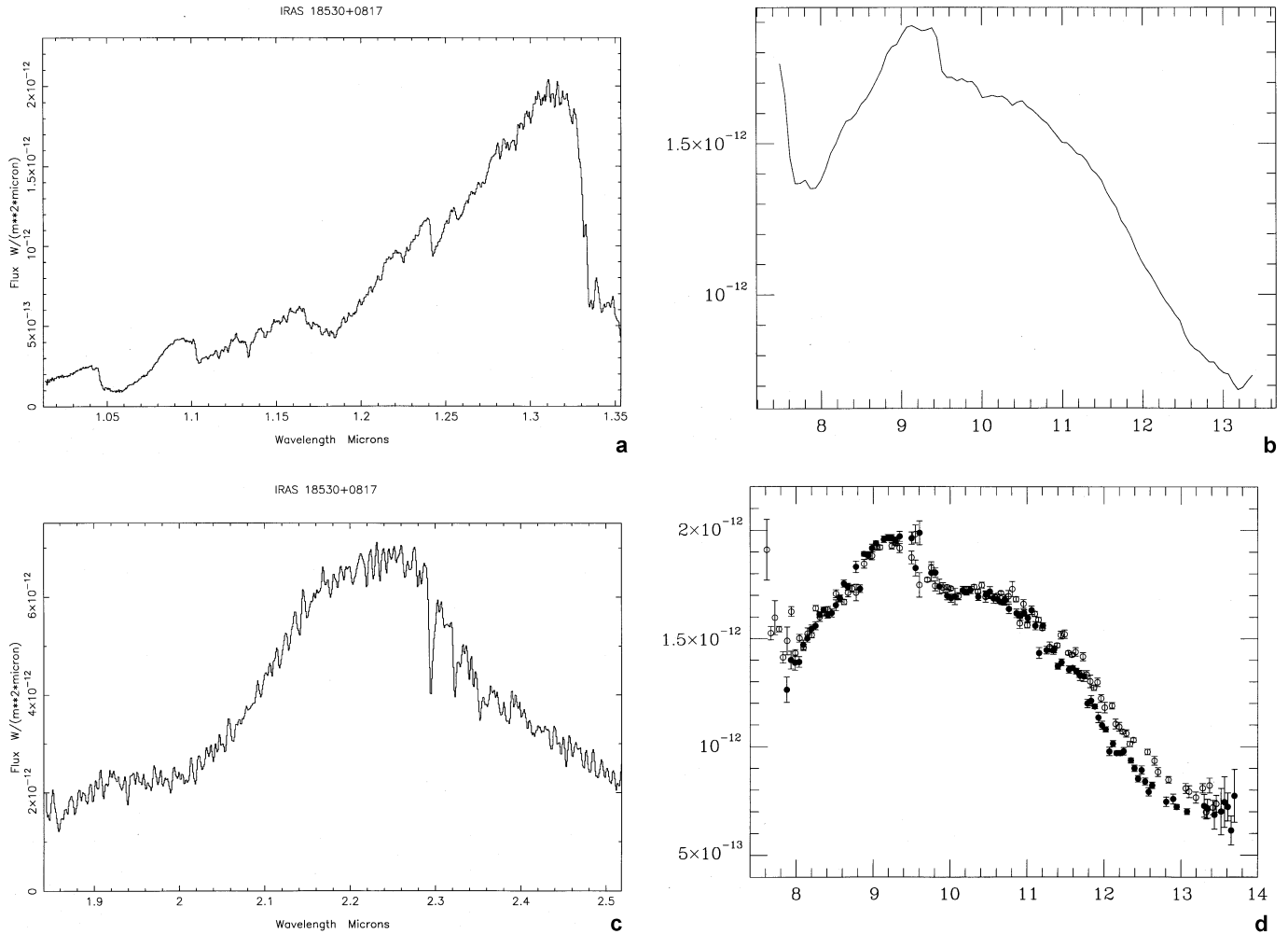


**Fig. 2a–d.** Spectra for IRAS 18530+0817. The unit of flux is  $\text{W m}^{-2} \mu\text{m}^{-1}$ . **a** UKIRT spectrum at 1.01 – 1.35  $\mu\text{m}$  **b** UKIRT spectrum at 7 – 13.5  $\mu\text{m}$  **c** UKIRT spectrum at 1.84 – 2.51  $\mu\text{m}$  **d** IRTF/HIFOGS spectrum at 7 – 13  $\mu\text{m}$ .

### 3.1. Photometry

In Table 2 we give the IRAS fluxes (with measurement error) at 12, 25, 60 and 100  $\mu\text{m}$  from co-added PASS2 CRDD, for the different UT-times during which the source was scanned, to illustrate the variability of the source. PASS2 CRDD were the IRAS survey data, recalibrated after the end of the mission, and with some instrumental effects removed. A further recalibration was performed by IPAC to produce PASS3 CRDD, the final IRAS survey data stream, but this recalibration did not change the relative variability effect reported here. The measurement error in Table 2 is a small part of the total error in the absolute value of the flux; this is dominated by calibration and other instrumental effects, see IRAS PSC Explanatory Supplement, 1987. We also give the IRAS LRS fluxes. The source is bright from 12 to 60  $\mu\text{m}$ , but it has a very weak and uncertain flux at 100  $\mu\text{m}$ . The IRAS data show significant flux variation in the 12 to 25  $\mu\text{m}$  range within a period of six months; there is no apparent flux variation at 60  $\mu\text{m}$ .

In Table 3 we show data from sources other than IRAS together with the IRAS PSC fluxes, firstly photometry at various

wavelengths, and then line observations. The source is not visible at R (0.7  $\mu\text{m}$ ); it is fainter than 19.0 magnitude, in agreement with the upper limit of Ghosh et al. (1984). It is detected at I (1.03  $\mu\text{m}$ ) with a magnitude of 16.1 (from the SAAO CCD observations). The observations of the EIC catalog (made in 1977) give a flux at 2.7  $\mu\text{m}$  (see Table 3). Fluxes at H, K, L, from Kastner et al. (1993) are also given in Table 3. These fluxes have no corrections because Kastner et al. could not estimate the distance. Loup et al. (1993) estimated the distance (1.9 kpc), by comparing the measured luminosity to an assumed standard luminosity.

### 3.2. J and K spectra

The J and K spectra of IRAS 18530+0817 are shown in Fig. 2a and 2c. The spectra are dominated by molecular absorption bands, most importantly by strong water bands centred at 1.4, 1.9 and 2.7  $\mu\text{m}$ . The latter two bands severely attenuate both the short and long wavelength portions of the K band. The water bands are prominent in very cool dwarfs (Jones et al., 1994) and

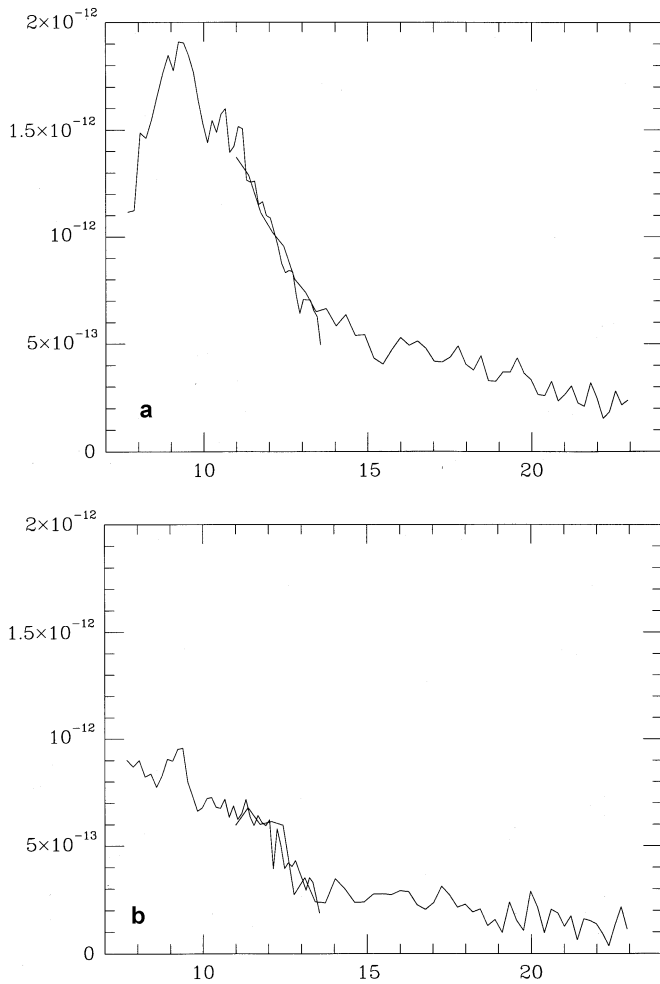


**Fig. 3a and b.** IRAS LRS spectra of the source IRAS 18530+0817, at 8 – 22  $\mu\text{m}$ . The unit of flux is  $\text{W m}^{-2} \mu\text{m}^{-1}$ . The first spectrum **a** was taken near the beginning of the IRAS survey and the second **b** about six months later.

in red giants, especially Mira variables (e.g. Johnson & Mendez, 1970; Strecker et al., 1978). The large  $10\mu\text{m}$  flux and strong dust emission feature imply that IRAS 18530+0817 is a giant rather than a dwarf. Using the ratio of  $2.2\mu\text{m}$  to  $1.9\mu\text{m}$  flux densities as an indicator, the  $1.9\mu\text{m}$  water band in IRAS 18530+0817 is stronger than that of any known Mira variable.

Strong  $^{12}\text{CO}$  absorption band heads at  $2.295\mu\text{m}$  ( $v=2-0$ ) and  $2.323\mu\text{m}$  ( $v=3-1$ ) are apparent in the K band spectrum. At  $2.352\mu\text{m}$  and  $2.383\mu\text{m}$ , the 4-2 and 5-3 bands can also be seen, but they are weak due to the low temperature of the photosphere and the increasing dominance of water at longer wavelengths. The first two band heads of  $^{13}\text{CO}$  can also be seen, at  $2.345\mu\text{m}$  and  $2.374\mu\text{m}$ . In the J band, the VO absorption centred at  $1.06\mu\text{m}$  and the band head of  $\text{H}_2\text{O}$  at  $1.33\mu\text{m}$  are particularly prominent. Many other weaker bands can be seen, as well as innumerable narrow lines, the discussion of which is beyond the scope of this paper.

### 3.3. $10\mu\text{m}$ spectra

The LRS spectra of IRAS 18530+0817 taken in 1983 by IRAS (Fig. 1a showing the mean spectrum and Fig. 3 showing two individual spectra, taken around 6 months apart) are featureless in the region 14 – 23  $\mu\text{m}$ , apart from the weak, broad silicate emission feature around  $18\mu\text{m}$ , with maximum flux density of about  $10^{-13} \text{W m}^{-2} \mu\text{m}^{-1}$ . The spectra (see Figs. 1a, 2b and 2d) are different in the region 8 – 12  $\mu\text{m}$  compared to those for many oxygen-rich stars, in that the silicate feature has an unusual shape compared to other  $10\mu\text{m}$  silicate emission features (see Fig. 1). The silicate feature peaks close to  $9\mu\text{m}$  and the feature appears to have either two components or mild self absorption. The self absorption of the silicate feature usually leaves the red wing of this emission feature peaked around  $11.4\mu\text{m}$  (see Fig. 1c), so that the red wing can look like a silicon carbide emission feature (Walker and Cohen, 1988). This is not seen here.

The spectrum taken with CGS3 at UKIRT in 1993 (Fig. 2b), from  $7.5\mu\text{m}$  to  $13.4\mu\text{m}$  show a silicate feature very similar to that seen in the LRS spectrum (e.g. Fig. 3a), but its higher spectral resolution and coverage at shorter wavelengths reveal additional information. There is a sharp drop in the flux of the emission feature at  $9.5\mu\text{m}$ , unresolved at the resolution of this spectrum ( $0.18\mu\text{m}$ ). The SiO fundamental band is more fully seen at the short wavelengths (Vardya et al., 1986), and the sharp edge at  $7.6\mu\text{m}$  is the 1-0 band head, which marks the onset of SiO absorption. The detection of the band head, which occurs at a rotational quantum number of about 125, demonstrates that the stellar photosphere is being detected at this wavelength.

The HIFOGS spectrum, obtained in June 1995 (Fig. 2d), is similar to the earlier CGS3 spectrum, except that the drop at  $9.5\mu\text{m}$  is more gradual. This shape has been confirmed by an almost simultaneous CGS3 observation and a CGS3 spectrum taken in August 1995 (not shown). They do not show the sharp drop at  $9.5\mu\text{m}$ , but show a smooth depression around  $1\mu\text{m}$  wide, centred at around  $9.7\mu\text{m}$ . This could be due to absorption by cooler circumstellar dust, silicate dust of a different composition, or by intervening dust grains along the line of sight. When the HIFOGS data are smoothed to a resolution similar to that of the IRAS LRS, and scaled in flux (Fig. 4), the shapes of the features observed by the two instruments are very similar, except that the drop is again less pronounced in the HIFOGS data.

## 4. Discussion

The presence of the strong molecular bands of SiO and  $\text{H}_2\text{O}$  show that the object is oxygen-rich. This is consistent with the emission feature at  $9\mu\text{m}$  being due to silicates. The spectral observations around  $2\mu\text{m}$  show two deep CO absorption bands, at  $2.925\mu\text{m}$  and  $2.323\mu\text{m}$  (the  $^{12}\text{CO}$  (2,0) and (3,1) band heads). Using Kleinmann and Hall (1986), the star is classified as a late M giant or supergiant, owing to the deep CO bands. The strong water bands imply that the star is a red giant, probably a Mira variable, and the great depth of the  $1.9\mu\text{m}$  band (discussed earlier) argues that the object is of a later spectral type than any

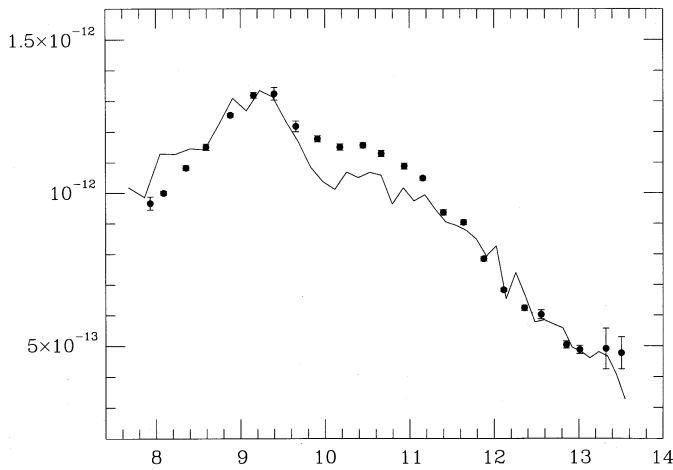


**Fig. 4.** Comparison of  $10\mu\text{m}$  spectra of IRAS 18530+0817. The HI-FOGS spectrum smoothed to a resolving power of 20–60, and scaled in flux is shown by filled circles. The mean IRAS LRS spectrum is plotted as a solid line. The unit of flux is  $\text{W m}^{-2} \mu\text{m}^{-1}$ .

previously observed Mira variable. Lewis et al. (1990) found that only the brightest stars were detected in the OH molecule, so that although the system contains water the absence of detectable OH is not surprising in view of the distance of the star (1.9 kpc according to Loup et al., 1993; although this distance is uncertain because they used a standard luminosity for their sample).

The IRAS colours from the  $12/25/60 \mu\text{m}$  data show the star to be a late O-rich star with a moderate dust shell. The colours ( $[12] - [25] = 1.30$ ,  $[25] - [60] = -0.06$ ), using Walker et al. (1989) place the system on the extreme red edge of the region of O-rich stars with silicate emission and the region of O-rich stars with silicate absorption. These stars are mostly Miras and other AGB stars. Using Van der Veen and Habing (1988), their IRAS colours ( $[12] - [25] = -0.26$ ,  $[25] - [60] = -1.93$ ) put the source in region IIIa (variable stars with more evolved O-rich circumstellar shells), close to the “evolutionary track”. The IRAS colours are consistent with the conclusion from the spectra that the star is a late type Mira variable.

The source IRAS 18530+0817 has an IRAS likelihood of variability  $>90\%$ , indicating significant variation of 12 and  $25\mu\text{m}$  fluxes with time. In Table 2 we see that the source remained relatively constant during a time interval of a few days (8 days) but showed a large flux decrease six months later, towards the end of the survey. Soon after there is possibly a further flux decrease, this one within a 26 hour time-interval. We observe a similar decrease in the IRAS LRS spectra shown in Fig. 3. The spectrum in Fig. 3a was taken near the beginning of the survey, the spectrum in Fig. 3b was taken about six months later and there is a large decrease in energy output as well as changes in the morphology of the spectrum. The bright emission feature at  $9.5\mu\text{m}$  remains relatively unaltered whereas the emission component around  $11\mu\text{m}$  has almost disappeared.

Ground-based spectra in the  $10\mu\text{m}$  window are generally uncertain in the  $9.4\mu\text{m} - 10.0\mu\text{m}$  region, due to the difficul-

ties in correcting for the strong telluric ozone absorption band at around  $9.7\mu\text{m}$  (note the larger error bars for the affected data points in Fig. 2d). Thus the unresolved absorption edge at  $9.5\mu\text{m}$ , present in the CGS3 spectrum (Fig. 2b), should be questioned, especially since it was not seen subsequently by CGS3 or HIFOGS. However, the consistency of the shift in flux level longward and shortward of  $9.5\mu\text{m}$  in this spectrum, which is composed of three sub-spectra shifted by  $1/3$  resolution element and obtained sequentially in time, is strong evidence that the feature is real. Moreover, the shape of the IRAS LRS spectrum is consistent with the CGS3 spectrum in Fig. 2b and with the smoothed HIFOGS spectrum in Fig. 4a.

It may be that IRAS 18530+0817 has a mild silicate self-absorption feature, but it does not appear very similar to other examples. The unusual shape could be caused by an unknown absorption feature. Sequences of CGS3  $10\mu\text{m}$  spectra of Mira and IK Tau (a very cool Mira variable) were examined; they showed SiO absorption near  $8\mu\text{m}$  and smooth silicate emission profiles, but no silicate self-absorption or sharp absorption features, such as the one at  $9.5\mu\text{m}$  seen in IRAS 18530+0817. We have not been able to identify the absorber responsible for the feature. The edge could be the band head of an unidentified molecule that becomes prominent at a certain phase in the period of IRAS 18530+0817.

Another alternative is that the feature (and its variability) could be an unusual manifestation of circumstellar silicate absorption in this object. Stars, with conventional  $10\mu\text{m}$  silicate features, sometimes show slight evidence of structure in the feature around  $10 - 10.5 \mu\text{m}$  (e.g. Tielens, 1990; Barlow, 1993). Tielens (1990) suggested that some Miras have silicates other than the usual astronomical silicate (olivine) present. He proposed the presence of disordered silicates (also oxides) but these mainly influence the shape longward of  $9.7\mu\text{m}$ . Bradley et al. (1992) have an interesting alternative, from their work on Interplanetary Dust Particles (IDPs). Some of their samples have a strong emission component around  $9\mu\text{m}$ . It would appear that a mixture of olivine (normal astronomical silicate) with some pyroxene could explain the unusual shape of IRAS 18530+0817. Alternatively, the glass-rich IDPs, which produced silicate features similar to comets Halley and Bradfield, also have quite a conspicuous  $9\mu\text{m}$  component to their broad silicate feature.

We conclude that although the central star of IRAS 18530+0817 may appear to be a normal very-late Mira star (with perhaps the coolest photosphere yet detected in such stars), the dust around it is somewhat unusual. The shape of the  $9\mu\text{m}$  feature appears to vary, apparently cut off by an absorption edge at  $9.5\mu\text{m}$  at some times, and is partly self-absorbed at other times. Features may arise from the presence of dust which is similar to interplanetary dust, in addition to the normal astronomical silicate dust shell.

*Acknowledgements.* We are grateful to the staffs of UKIRT and IRTF for their support of these observations. Some of the data presented here were obtained with the UKIRT Service programme. UKIRT is operated by the Joint Astronomy Centre on behalf of the UK Particle Physics and Astronomy Research Council (PPARC). Some of the data reduction was undertaken on the Starlink Network, which is run by

the Central Laboratory of the Research Councils (CLRC) on behalf of PPARC. One of us (VT) gratefully acknowledges RAL's financial support. We are grateful to the referee for helpful comments on the paper.

## References

- Barlow, M.J., 1993. In "Astronomical Infrared Spectroscopy: Future Observational Directions", ed. S. Kwok, *Ast. Soc. Pacific Conf. Ser.* 41, 97
- Bradley, J.P., Humecki, H.J. and Germani, M.S., 1992. *ApJ* 394, 643
- Cheeseman, P., Stutz, J., Matthew, S., Taylor, W., Goebel, J., Volk, K. and Walker, H., 1989. NASA Reference Publication 1217, Washington D.C.
- Ghosh, S.K., Iyengar, K.V.K., Rengarajan, T.N., Tandon, S.N., Verma, R.P. and Daniel, R.R., 1984. *MNRAS* 206, 611
- IRAS Science Team, 1986. IRAS Low Resolution Spectra Atlas, *A&AS* 65, 607
- IRAS Science Team, 1987. IRAS Point Source Catalog, JPL Publication
- Johnson, H.L. & Mendez, M.E., 1970. *AJ* 75, 785
- Jones, H.R.A., Longmore, A.J., Jameson, R.F. & Mountain, C.M., 1994. *MNRAS* 267, 413
- Kastner, J.H., Forveille, T., Zuckerman, B. and Omont, A., 1993. *A&A* 275, 163
- Kleinmann, S.G. & Hall, D.N.B., 1986. *ApJS* 62, 501
- Lewis, B.M., Eder, J. and Terzian, Y., 1990. *ApJ* 362, 634
- Loup, C., Forveille, T., Omont, A. and Paul, J.F., 1993. *A&AS* 99, 291
- Sweeney, L.H., Heinsheimer, T.F., Yates, F.F., Maran, S.P., Lesh, J.R. and Nagy, T.A., 1978. Interim Equatorial Infrared Catalogue, TR-0078 (3409-20)-1 (Los Angeles: The Aerospace Corporation)
- Strecker, D.W., Erickson, E.F. & Witteborn, F.C., 1978. *AJ* 83, 26
- Tielens, A.G.G.M., 1990. In "From Miras to Planetary Nebulae", ed. M.O. Mennessier and A. Omont (Singapore: Fong and Sons), 186
- Tsikoudi, V., 1988. *AJ* 95, 1797
- Van der Veen, W.E.C.J. and Habing, H.J., 1988. *A&A* 194, 125
- Vardya, M.S., de Jong, T. and Willems, F.J., 1986. *ApJ Lett.* 304, L29
- Walker, H.J. and Cohen, M., 1988. *AJ* 95, 1801
- Walker, H.J., Cohen, M., Volk, K., Wainscoat, R.J. and Schwartz, D.E., 1989. *AJ* 98, 2163
- Witteborn, F.C., Bregman, J.D., Rank, D.M. and Cohen, M., 1991. In "Proc. of the 1991 North American Workshop on Infrared Spectroscopy", ed. R.E. Stencel (Boulder: Univ. Colorado), 29